JOURNAL OF SOLID STATE CHEMISTRY **133,** 314–321 (1997)
ARTICLE NO. SC977493

Thermoelectric Properties of Boron and Boron Phosphide CVD Wafers

Y. Kumashiro, T. Yokoyama, A. Sato, and Y. Ando

Faculty of Engineering, Yokohama National University, 156 Tokiwadai, Hodogaya, Yokohama 240, Japan

Received May 19, 1997; accepted May, 27, 1997

Electrical and thermal conductivities and thermoelectric power of *p*-type boron and *n*-type boron phosphide wafers with amorphous and polycrystalline structures were measured up to high temperatures. The electrical conductivity of amorphous boron wafers is compatible to that of polycrystals at high temperatures and obeys Mott's $T^{-1/4}$ rule. The thermoelectric power of polycrystalline boron decreases with increasing temperature, while that of amorphous boron is almost constant in a wide temperature range. The weak temperature dependence of the thermal conductivity of BP polycrystalline wafers reflects phonon scattering by grain boundaries. Thermal conductivity of an amorphous boron wafer is almost constant in a wide temperature range, showing a characteristic of a glass. The figure of merit of polycrystalline BP wafers is 10^{-7}/K at high temperatures while that of amorphous boron is 10^{-5}/K. © 1997 Academic Press

INTRODUCTION

Boron-based semiconductors are refractory semiconductors and are divided into two categories, i.e., boron rich semiconductors derived from four crystalline boron modifications and III–V compound semiconductors like BP and BAs. One of their common characteristics is the high thermoelectric power, which is promising for high-temperature thermoelectric devices with high-efficiency thermoelectric energy conversion (1). The formation of *p–n* junctions is preferable to thermoelectric devices, but there exist some problems.

Undoped boron is *p*-type and it is very difficult to prepare *n*-type boron-rich semiconductors by doping(2–4). As for boron phosphide, its single crystalline wafer has high thermoelectric power (5, 6), but thermal conductivity is also high (7, 8), which reduces the thermoelectric figure of merit of 1×10^{-8}/K (9). The thermal conductivity of sintered BP polycrystals (10) is smaller than that of single crystalline wafers, which would expected to increase the figure of merit. However, thermoelectric power of BP sintered specimens depends on the purity of the starting powder (9). We have obtained high thermoelectric power and high figures of merit by using high-purity BP powder prepared by hydroisostatic pressing (9). In this case it is very difficult to obtain an *n*-type BP sintered specimen.

We have chosen polycrystaline and amorphous boron for *p*-type materials and BP polycrystalline wafers for *n*-type materials as a first step to study the thermoelectric device. For this purpose, we have prepared polycrystal and amorphous boron and boron phosphide wafers by chemical vapor deposition (11, 12) and clarified their thermoelectric properties, i.e., electrical conductivity, thermoelectric power, and thermal conductivity up to high temperatures.

EXPERIMENTAL

The preparation of wafers was performed on Si(100) and fused silica glass substrate by thermal decomposition of B_2H_6 (1% in hydrogen) and PH_3 (5% in hydrogen) under a hydrogen atmosphere(12). The reaction chamber was made of fused quartz with the upper part cooled by running water. The preparation was made at gas-flow rates of 20–60, 300, and 2500 sccm for diborane, phosphine, and hydrogen, respectively, in optimum temperatures at deposition times of 20–28 h. The film growth experiment for 1.5 h was used to determine optimum growth conditions for wafers. The wafers were obtained by solving away the Si substrate in $HF–HNO_3$ solution.

The quality of the specimen was evaluated by X-ray diffraction and SEM observation.

Ohmic contacts of the films were made by evaporated Al, followed by annealing in argon at 400°C for 1 h. Electrical properties of the specimen at room temperature were measured by the van der Pauw method. A block diagram of the apparatus for thermoelectric measurement is found in (13, 14). Electrical conductivity of the films were measured by a two-terminal method at temperature between room temperature and 800°C under argon atmosphere. Thermoelectric voltage between hot and cold junctions was measured under a constant temperature gradient of 2–3°C.

The thermal diffusivity of wafers was measured by the laser flash method using a ring flash light (7, 8), which originates from multi-variable analysis in a two-dimensional model. Graphite-coated thin films with a thickness of

0022-4596/97 $25.00

~5 μm were sprayed onto both faces of the specimen with a dry graphite film lubricant (dgf 123 produced by Japan Ship Machine Tool Company Limited).

Thermal conductivity was calculated from the measurement of thermal diffusivity and the data on heat capacities of BP single crystal (8) and amorphous boron (15).

RESULTS AND DISCUSSION

A. Preparation of Films

The morphology and crystality of the boron film on the Si(100) plane depends on the substrate temperature (Table 1). The films grown on the substrate temperatures of 700–1050°C are amorphous, while that grown on the substrate temperature of 1150°C becomes polycrystaline through the mixture of amorphous and polycrystals grown at 1100°C. The color of the amorphous films are gray and change from black gray to black in color in the progress of crystallization from amorphous to polycrystal. The growth rates increase with the rise in substrate temperature according to the Arrhenius rule in the amorphous region and become independent of temperature in the polycrystal region. X-ray diffraction patterns of the films excluding the peaks of Si are shown in Fig. 1. The films grown at temperatures of 700–1050°C show only a characteristic broad peak near $2\theta = 20$. The film grown at 1100°C consists of an α-rhombohedral (322) plane, weak α-tetragonal (200) and (400) planes, and a broad peak. The broad peak would consist of an α-rhombohedral (111) plane and an α-tetragonal (202) plane, lessening crystal quality. The film grown at 1150°C is polycrystalline with strong peaks of α-rhombohedral (111) and (322) planes. Also the peaks of α-tetragonal (200), (202), (222), and (400) planes are observed, but they are a few percent of the highest peak of α-rhombohedral (111), plane, showing nearly α-rhombohedral monophase structure. That at 1200°C tends to grow α-tetragonal structure with the mixtures of α-rhombohedral and tetragonal structures, which is the transient region from α-rhombohedral to α-tetragonal structure in increasing growth temperature. SEM observations of these films (Fig. 2) indicate that the characteristic hemisphere in shape with a diameter of 1–2.5 μm in the amorphous films grown at 700°C disappears in that grown above 1150°C with fine grains of 0.5–1 μm due to the formation of the α-tetragonal phase. The film grown at 1100°C shows coexistance of grain particles and aggregation of hemispheres. X-ray diffraction suggests that the small crystallites would be α-rhombohedral and tetragonal structures. The crystal grains become fine at the growth temperature of 1200°C and the shape of the grain is somewhat different from that at 1150°C arising from the formation of the α-tetragonal structure.

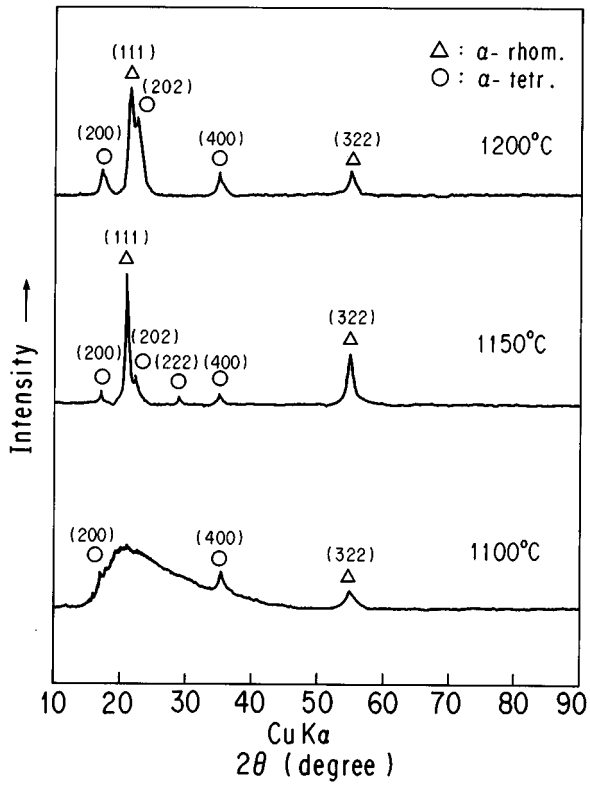

FIG. 1. X-ray diffraction patterns from boron films on the Si(100) surfaceat various substrate temperatures.

Table 1
Features of Boron Films on the Si(100) Plane for the Deposition Time of 1.5 h

Deposition temperature (°C)	Growth rate (μm/h)	Structure	Surface
700	1.6	Amorphous	Gray
800	1.9	Amorphous	Gray
900	2.5	Amorphous	Gray
950	2.6	Amorphous	Gray
1000	2.8	Amorphous	Gray
1050	2.8	Amorphous	Gray
1100	2.9	Polycrystal and amorphous	Black–gray
1150	3.1	Nearly α-rhom.	Black–gray
1200	3.1	α-rhom and-α-tetr	Black

In contrast, boron films grown on fused silica glass at the temperatures 700–1000°C show amorphous X-ray diffraction patterns characterized by a broad peak near $2\theta = 20°$. SEM analyses of the films indicate that the films grown below 900°C have uniform hemispherical particles 1–2 μm in diameter and those grown at 950–1000°C consist of two different particles of 1–2 and 3–5 μm in diameter. Especially those grown at 1100°C have cracks and are not uniform.

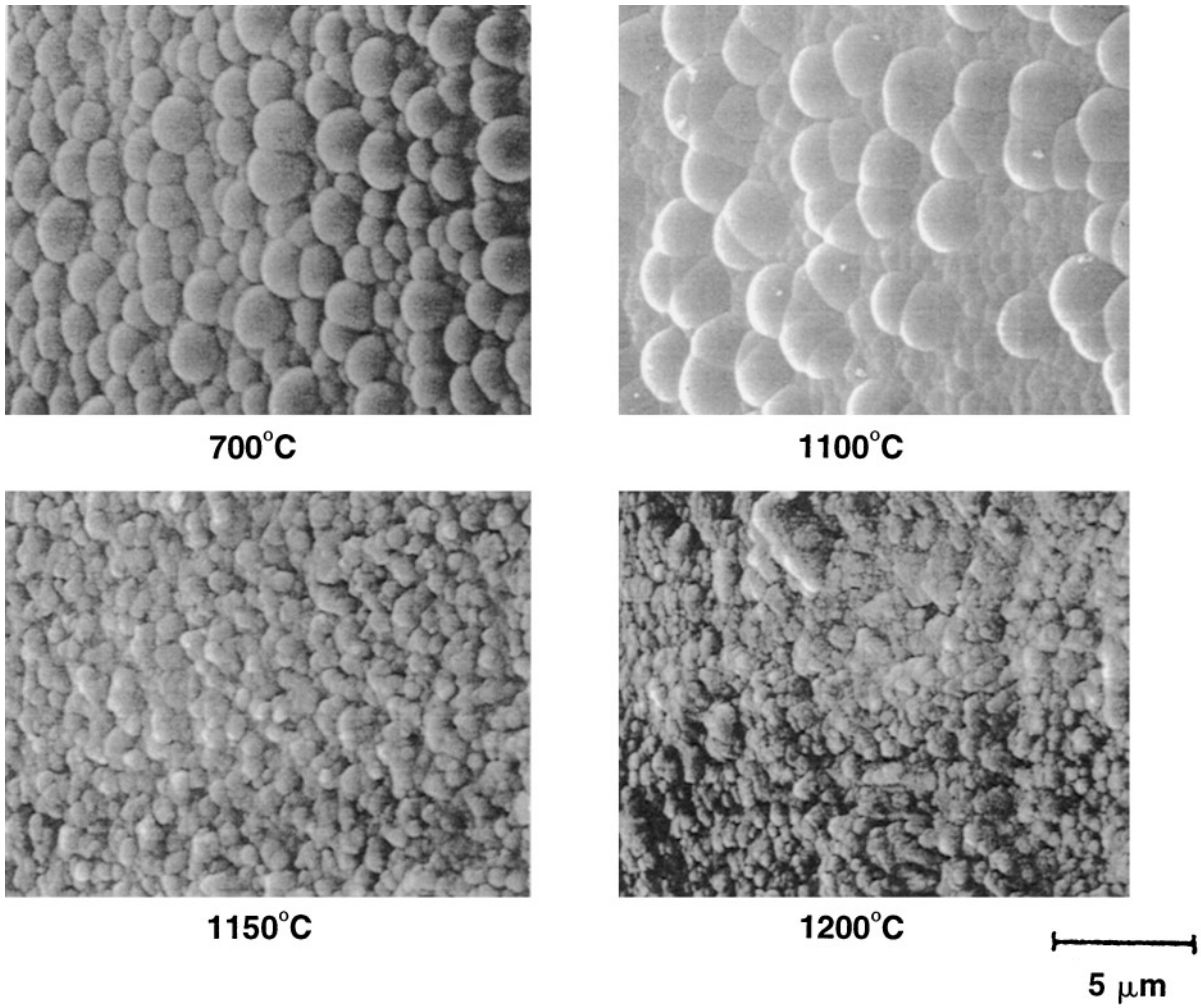

FIG. 2. SEM images of the boron layers at various substrate temperatures.

Electrical properties of boron films on fused silica glass are shown in Table 2. All films show *p*-type conductors. With an increase in the growth temperatures, the electrical resistivity tends to increase and hole concentration decreases, but they become almost constant at above 900°C. However, surface smoothness and homogeneous deposition of the film on 900°C is better than that on 950°C.

TABLE 2
Electrical Properties of Boron and Boron Phosphide Films on Silica Glass

Film	Substrate temperature (°C)	Resistivity (Ω cm)	Carrier concentration (cm^{-3})	Mobility ($cm^2/V\,s$)	Conduction type
B	700	8.8×10^4	2.7×10^{13}	24.5	
	800	2.3×10^4	1.0×10^{13}	27.0	
	850	6.2×10^4	5.5×10^{12}	28.2	*p*-type
	900	9.9×10^5	1.8×10^{12}	29.7	
	950	9.8×10^5	2.0×10^{12}	28.8	
BP	800	51.3	9.5×10^{15}	12.7	*n*-type

The features of the BP films on the fused silica glass substrate are summarized in Table 3. The films grown at 700°C look reddish-black but powders also deposit onto the surface of the film. Those at 900°C have some some cracks on the surface. Those at 1000°C are black–gray in appearance, lacking a smooth surface. The film grown at 800°C is reddish-black in color with a smooth surface. Growth rates of the films are nearly constant at 6–8 μm/h.

X-ray diffraction patterns of the BP films with monophases are shown in Fig. 3. The diffraction patterns of films grown at 700°C have a broad peak at the low-angle side corresponding to an amorphous state and other peaks are not so sharp, indicating mixtures of amorphous and polycrystalline phases. X-ray diffraction patterns of the homogeneous films grown at 800°C are similar to those at 700°C except for the amorphous peak; however, the film would

TABLE 3
Features of Boron Phosphide Films on Fused Silica Glass for the Deposition Times of 1.5 h

Deposition temperature (°C)	Growth rate (μm/h)	Structure	Surface
700	8.2	Polycrystal and partially amorphous	Reddish black and partially powder
800	8.5	Polycrystal with oriented to (111), (100) planes	Reddish black with smooth surface
900	7.2	Polycrystal	Reddish black and crack
1000	5.7	Polycrystal	Black–gray with rough surface
1100	6.1	Polycrystal and compound of Si	Red brown

grow with the orientation of the (111) plane or the (100) plane to some extent. The films grown at 900 and 1000°C change the diffraction pattern from those at 800°C with decreasing peak height, showing the deterioration of crystal quality.

The SEM analyses (Fig. 4) of the films grown at 700°C consist of two different phases of amorphous and polycrystals and cracks exist between the two phases with poor crystalinity. The films grown at 800°C consist of very fine crystal grains with smooth surfaces but those grown at 900°C have irregular surface scatter in the crystal grain. The films grown at 1000°C show different morphology from other films with large crystal grains of ~8 μm and rough surface. Because of inhomogeniety and cracks in the film, the electrical properties of BP films except for those grown at 800°C which give *n*-type behavior, (Table 2) could not be measured.

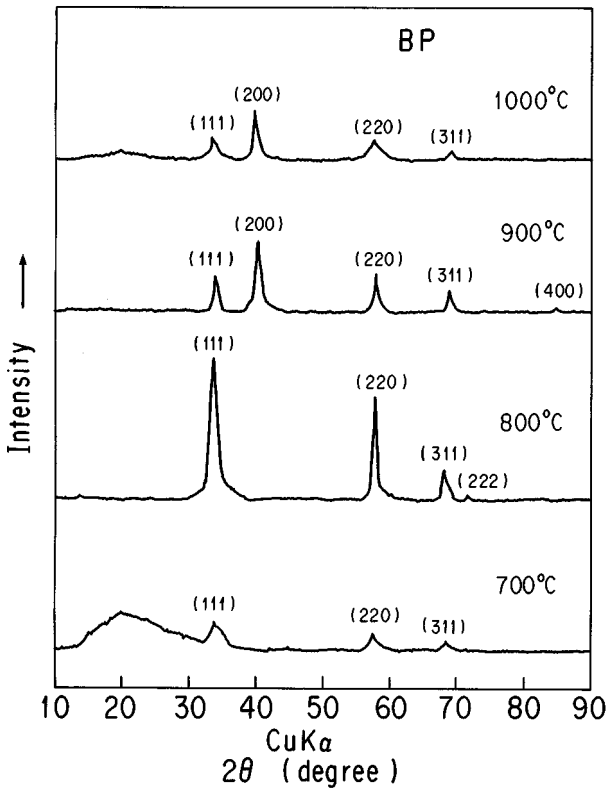

FIG. 3. X-ray diffraction patterns from boron phosphide films on fused silica glass at various substrate temperatures.

B. Preparation of Wafers

The boron and boron phosphide polycrystal and amorphous wafers were prepared in accordance with growth conditions for the films. However, boron wafers were not prepared on the silica glass substrate where the crack was initiated at the entire range during the long time growth experiment to break the wafers into some pieces. Then boron wafers were prepared on the Si(100) plane at temperatures of 1050 and 1100°C for amorphous and polycrystalline wafers, respectively. The Si substrates with the B layers were distorted to form a convex shape with the B layer outside, when cooled to room temperature after the long time experiment of ~20 h. The distortion brings on the generation of cracks in B. Boron wafers with an area of $10 \times 11\ mm^2$ and a thickness of 50–60 μm were obtained by dissolving away the silicon substrate in an $HF–HNO_3$ solution.

A boron phosphide wafer ($10 \times 20\ mm^2$, 200 μm in thickness) was grown on the silica glass at 800°C for ~20 h and was peeled easily from the substrate after the long time growth without any chemical treatment. However, long time growth at 900°C for BP initiated many cracks during the growth process.

X-ray diffraction patterns and SEM observations of these boron and boron phosphide wafers are almost similar features to those of films in Section A, indicating that crystal quality would be preserved even for long time growth.

The electrical properties of these wafers are shown in Table 4. No appreciable differences between film and wafer for BP is found, but a large discrepancy exists for boron except for electrical resistivity owing to the substrate. A boron wafer grown on Si substrate contains autodoped Si from the substrate with the concentration of

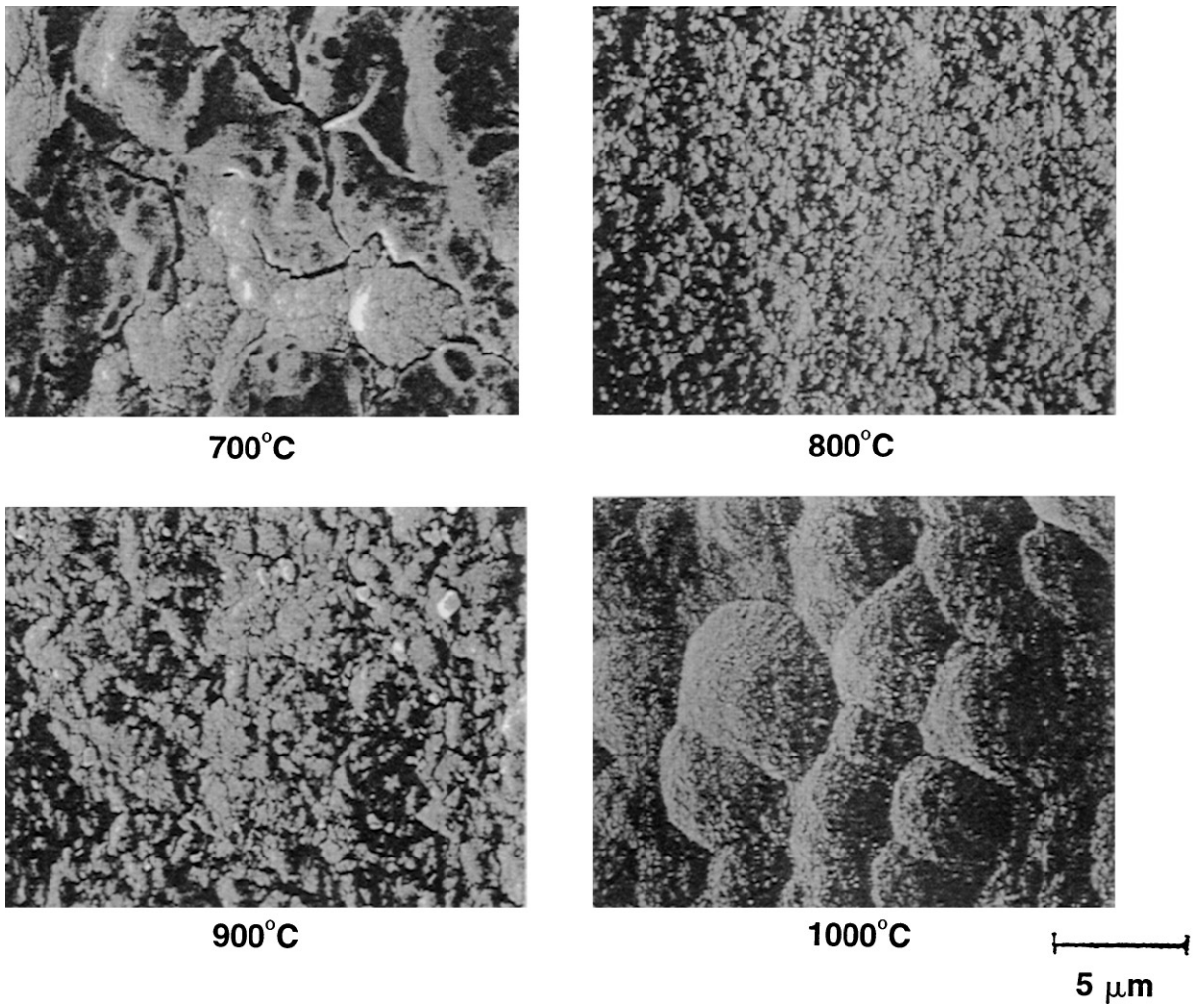

FIG. 4. SEM images of the boron phosphide surface at various substrate temperatures.

10^{20}–10^{21} atoms/cm^3 which increases the carrier concentration as acceptors, so that mobility would reduce by impurity scattering. High resistivity is characteristic of amorphous materials and reduces from amorphous to crystal. Also low mobility, less than 1 cm^2/v s for the amorphous boron wafer, indicates "quasi-amorphous" semiconductor characterized hopping conduction (16).

TABLE 4
Electrical Properties of Boron and Boron Phosphide Wafers

Wafer	Resistivity (Ωcm)	Carrier concentration (cm^{-3})	Mobility (cm^2/V sec)	Conduction type
Amorphous B	1.31×10^4	$\sim 10^{16}$	$10^{-2} \sim 10^{-3}$	*p*
Polycrystalline B	5.32	1.1×10^{18}	1.1	*p*
Polycrystalline BP	53.5	1.3×10^{16}	8.6	*n*

C. Thermoelectric Properties

Temperature dependencies of electrical conductivity (σ) for boron and boron phosphide are shown in Fig. 5. The data include conductivity of an α-rhombohedral boron polycrystal (16). By applying $\log \sigma$ vs $1/T$ for amorphous boron, we obtained 0.6 eV, which is smaller than other amorphous films (13). The relationship between $\log \sigma$ and $1/T$ is slightly concave, but $\log \sigma$ vs $T^{-1/4}$ is linear, which is explained by a hopping conduction (1).

In contrast, the conductivity of the crystalline boron wafer shows a gradual increase up to 800 K, above which it increases steeply with temperature to induce the activation energy of 1.5–1.6 eV, being nearly the band gap of α-rhombohedral boron of 1.9 eV (16) (Fig. 5). The intrinsic conduction would begin to appear at high temperature, so that thermal activated band conduction would be applicable.

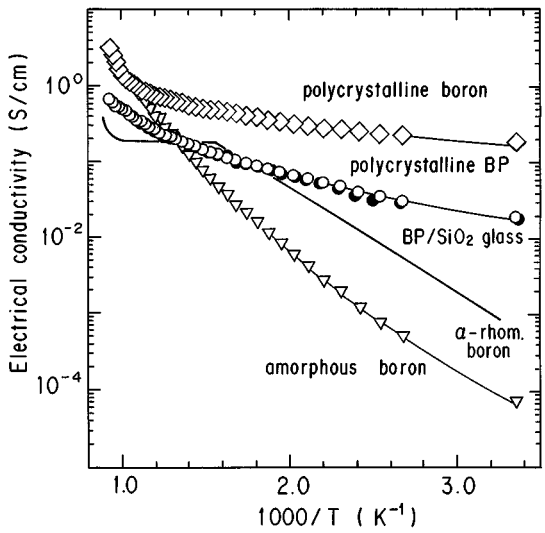

FIG. 5. Temperature dependence of conductivity of boron and boron phosphide. The result of α-B polycrystal (16) is also shown.

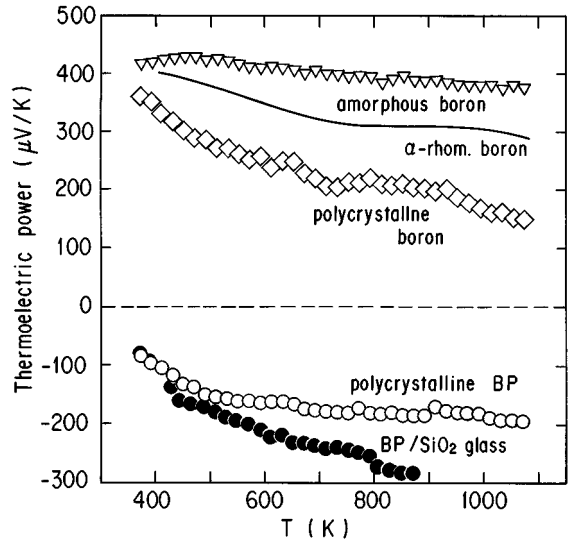

FIG. 6. Temperature dependence of thermoelectric power of boron and boron phosphide. The result of α-B polycrystal (2) is also shown.

Boron phosphide also shows a steep raise at 900 K. The activation energy at lower temperatures is 0.08 eV, corresponding to the doubly charged phosphorus (P^{++}) (6). Low carrier concentration (Table 4) would produce a steep rise in the electrical conductivity at high temperature with the activation energy of 0.3 eV, which would be due to the formation of impurity states and crystal defects and contribution to conduction by the excitation of carrier trapped by impurities and defect levels (17). No appreciable differences in electrical conductivity between film and wafer for BP is observed, which would extend to electrical properties at room temperature (Tables 2 and 4).

Temperature dependencies of thermoelectric power (α) are shown in Fig. 6, which includes α-rhombohedral boron polycrystal (2). The signs are consistent with the Hall effect (Tables 2 and 4). The smaller carrier concentration (Table 4) has the larger thermoelectric power for the boron specimen. The thermoelectric power of polycrystalline boron and α-rhombohedral boron crystal decrease, with increasing temperature in a similar way.

In contrast, the amorphous boron wafer shows unusual behavior of almost constant thermoelectric power for the entire temperature range. However, the thermoelectric power of highly disordered boron carbide (18) increases with the increase in the temperature explained by polaron hopping systems in which disorder is present in the hopping sites. By applying these phenomena to the present amorphous boron wafer we would expect an increase of the α value and an increase with the increase in temperature by an additional term representing the entropy associated with the transport of vibrational energy with hopping carriers the more disordered amorphous states are introduced into the wafer.

The absolute thermoelectric power for boron phosphide increases with increasing temperature. The α value of the wafer is almost constant between 600 and 1100 K while BP/SiO_2 increases with increasing T. This behavior is similar to that of a single crystalline wafer (5, 6), indicating that electron concentration ranges in the impurity region and Fermi energy lowers by the electron supply from donor level with increasing temperature.

The absolute thermoelectric power of BP films is higher than that of wafers. The absolute thermoelectric power of our previous results (14) on BP films grown onto sapphire crystal under the same growth temperature as the present case is higher than that of the present BP film, which would be due to the difference in the melting point of the substrate; i.e., the higher the melting point, the less autodoped impurity. The present BP film would be contaminated by impurities from the silica glass. The absolute α value of BP on fused silica glass is higher than that of the BP wafer, which would be probably caused by a stress effect in the film.

Thermal diffusivity of the polycrystalline BP and amorphous B wafer are shown in Figs. 7 and 8, respectively, while that of crystalline boron wafer was not measured owing to the difficulty in growing a wafer large enough to be measured. The thermal diffusivity at room temperature of 0.06 cm^2/s decreases to 0.04 cm^2/s at 800 K for the BP wafer. This behavior is different from that of the single crystalline wafer (7, 8), where thermal diffusivity obeys the T^{-1} rule. The thermal diffusivity for the amorphous B wafer

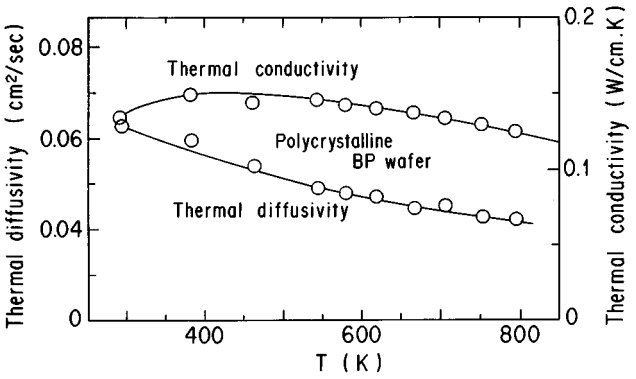

FIG. 7. Temperature dependencies of thermal diffusivity and thermal conductivity of BP polycrystal wafer.

(Fig. 8) exhibits a temperature dependence similar to the BP wafer.

Thermal conductivity (Fig. 7) is calculated by the product of the thermal diffusivity and the heat capacity of the single crystal (8). The density is calculated by the lattice constant. The thermal conductivity of the polycrystalline BP shows weak temperature dependence for the entire temperature range. Our previous result (10) on the thermal conductivity of sintered BP with the density of 60–65% of the theoretical value indicates an almost constant value of ~ 0.05 W/cm K for temperatures up to 800 K. The present thermal conductivity is higher than that of the sintered one's, but it is resonable when considering the porosity of the specimen. Then the thermal conduction is performed by phonon scattering at grain boundaries with weak temperature dependence of mean free path of phonons.

Thermal conductivity for the amorphous boron wafer is constant in a wide temperature range, showing characteristics of a glass as confirmed by Golikova *et al.*(19). For

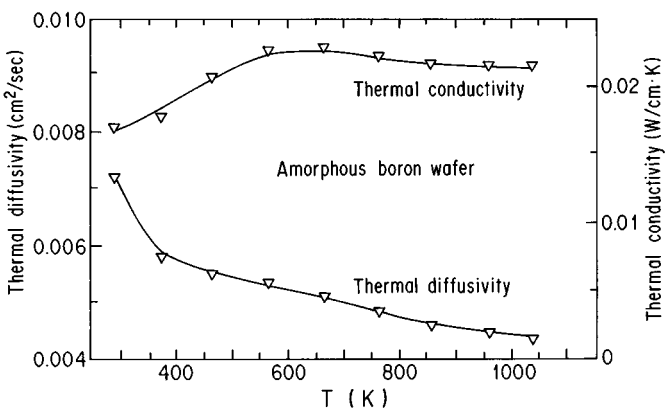

FIG. 8. Temperature dependencies of thermal diffusivity and thermal conductivity of amorphous B wafer.

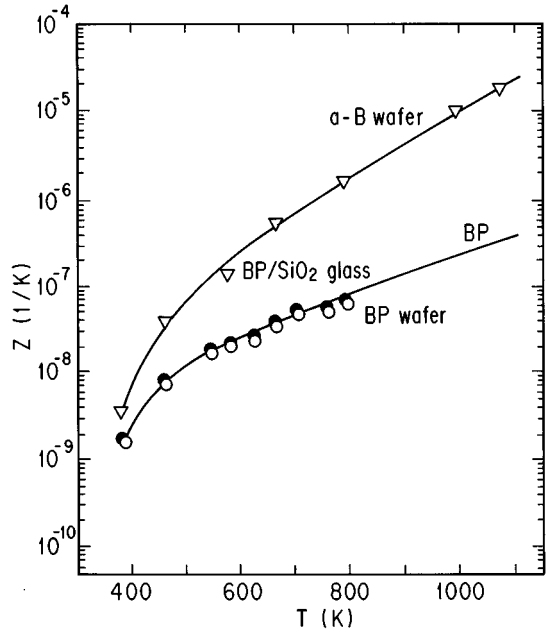

FIG. 9. Thermoelectric figure of merit for boron phosphide polycrystals and amorphous boron as a function of temperatures.

thermoelectric devices κ should be low to reduce the loss of thermal energy by thermal conduction between the hot and cold sides (1).

The efficiency of energy conversion of the thermoelectric device becomes high at larger figures of merit and at high temperature. The figure of merit is defined as

$$Z = \alpha^2\sigma/\kappa. \qquad [1]$$

The Z values for boron phosphide and amorphous boron are shown in Fig. 9. The Z value for the boron phosphide film is calculated by using the κ value for the present wafer. An increase in increasing temperature reaches $\sim 10^{-7}$/K at 800 K. However it would be $\sim 10^{-6}$/K if the thermal conductivity could be reduced as low as for the sintered specimen by introducing porosity and a disordered amorphous state. The Z values for the amorphous boron wafer increase with an increase in temperature and become $\sim 10^{-5}$ W/cm K at 1000 K, which are higher than those of the BP wafer by one order of magnitude. The $\alpha^2\sigma$ value for the crystalline boron wafer at low temperature is $\sim 10^{-8}$ W/cm K^2 owing to high carrier concentration and low electrical conductivity, but remains almost constant at high temperatures because of the competition of increasing electrical conductivity and decreasing thermoelectric power. The thermal conductivity of 0.05 W/cm K (20) at 1000 K for crystalline boron would produce the figure of merit of $\sim 10^{-7}$/K at 1000 K, being lower than those of the amorphous boron wafer by two order of magnitude.

CONCLUSION

We have prepared *p*-type amorphous and polycrystalline boron and *n*-type polycrystalline boron phosphide wafers by the CVD process and have measured electrical, thermal, and thermoelectrical properties of these specimens up to 1000 K. Though the thermoelectric figure of merit for boron phosphide is $\sim 10^{-7}$/K at high temperatures, it is possible to prompt up to 10^{-6}/K by introduction of a disordered state in the wafer. The figure of merit for amorphous boron is $\sim 10^{-5}$/K at high temperature while that for the polycrystal is estimated to be $\sim 10^{-7}$/K. A higher figure of merit would be expected by controlling structural and thermoelectric properties of these materials.

ACKNOWLEDGMENTS

This work is performed by the Thermal & Electric Energy Technology Foundation and Nippon Sheet Glass Foundation for Materials Science and Engineering.

REFERENCES

1. H. Werheit, *Mater. Sci. Eng. B* **29,** 228 (1995).
2. J. M. Dusseau and J. L. Robert, *J. Less-Common Met.* **82,** 137 (1981).
3. H. Werheit, K. De Groot, and W. Malkemper, *J. Less-Common Met.* **82,** 163 (1981).
4. G. A. Slack, J. H. Rosolowski, C. Hejna, M. Gabauskas, and J. S. Kasper, *in* "Proc. 9th Int. Symp. Boron, Borides and Related Compounds" (H. Werheit, Ed.), pp. 132. Universitat Duisburg Gesamthochschule, 1987.
5. S. Yugo, T. Sato, and T. Kimura, *Appl. Phys. Lett.* **46,** 842 (1985).
6. Y. Kumashiro, M. Hirabayashi, and T. Koshiro, *J. Less-Common Met.* **143,** 159 (1988)
7. Y. Kumashiro, T. Mitsuhashi, S. Okaya, F. Muta, T. Koshiro, Y. Takahashi, and M. Hirabayashi, *J. Appl. Phys.* **65,** 2147 (1989).
8. Y. Kumashiro, T. Mitsuhashi, S. Okaya, F. Muta, T. Koshiro, M. Hirabayashi, and Y. Okaya, *High Temp.-High Press.* **21,** 105 (1989).
9. Y. Kumashiro, M. Hirabayashi, and S. Takagi, *Mater. Res. Soc. Symp. Proc.* **162,** 585 (1990).
10. Y. Kumashiro, M. Hirabayashi, T. Koshiro, and Y. Takahashi, *in* "Sintering '87" (S. Somiya, M. Shimada, M. Yoshimura, and R. Watanabe, Eds.), pp. 43. Elsevier Appl. Soc., Amsterdam, 1987.
11. M. Takigawa, M. Hirayama, and K. Shono, *Jpn. J. Appl. Phys.* **12,** 1504 (1973).
12. Y. Kumashiro, Y. Okada, and H. Okumura, *J. Crystal Growth* **132,** 611 (1993).
13. K. Nakamura, *J. Electrochem. Soc.* **131,** 2691 (1984).
14. Y. Kumashiro, T. Yokoyama, J. Nakamura, K. Matsuda, and J. Takahashi, *Mater Res. Soc. Symp. Proc.* **242,** 629 (1992).
15. S. S. Wise, J. L. Margrave, and R. L. Altman, *J. Phys. Chem.* **64,** 915 (1960).
16. O. A. Golikova and S. Samatov, *Phys. Stat. Solidi* (*a*) **77,** 449 (1983).
17. S. Yugo and T. Kimura, *Phys. Stat. Solidi.* (*a*) **59**, 363 (1980).
18. T. L. Aselage, *Mater Res. Soc. Symp. Proc.* **234**, 145 (1991).
19. O. A. Golikova and A. Tadzhiev, *J. Non-Cryst. Solids* **87,** 64 (1986).
20. G. A. Slack, D. W. Oliver, and F. H. Horn, *Phys. Rev. B* **4,** 1714 (1971).